

# Fast optical re-phasing of segmented primary mirrors

Henri Bonnet<sup>\*a</sup>, Michael Esselborn<sup>a</sup>, Nick Kornweibel<sup>a</sup>, Philippe Dierickx<sup>a</sup>

<sup>a</sup>European Southern Observatory, Karl-Schwarzschild Straße 2, D-85748 Garching bei München, Germany

## ABSTRACT

For highly segmented primary mirrors, as that of the European Extremely Large Telescope (E-ELT) with its 798 segments, the capability to update regularly the optical phasing solution is essential for robust operations. The duration of standard phasing procedures is driven by the difficulty of maintaining the registration of the image of the primary on the phasing sensor with tolerances of  $\sim 0.02\%$  of the mirror diameter. The paper describes a re-phasing procedure with a dynamic range of about  $\pm 1.5$  microns. This is based on a standard Shack-Hartmann phasing sensor operated at 2 narrow bands filters with wavelength separation of 30%. Controlled registration offsets are applied during the acquisitions, allowing the registration parameters to be estimated from the phasing data. The procedure has been successfully validated at the Gran Telescopio de Canarias (GTC).

**Keywords:** Wavefront Control, Segmented Mirrors, Phasing

## 1. INTRODUCTION

The 798 segments of the primary mirror of the E-ELT are controlled in position by means of position actuators capable of adjusting the piston and tip-tilt relative to the local normal to the mirror. Edge Sensors measure the relative displacements of adjacent segments. Displacements are measured along the local normal (Piston direction) and the local mirror tangent plane (Gap and Shear direction). The optical phasing procedure aims at defining the set point of the Edge Sensors along the piston direction, with an accuracy of about 30nm in wavefront (spatial RMS of the inter-segment wavefront discontinuity), in order to bring the figure of the mirror to its prescription within tolerances. Thereafter, the intersegment piston and tip-tilt is held through the Edge Sensors until the next optical phasing.

The E-ELT baseline procedure for phasing was initially inherited from the 36-segments Keck telescope<sup>[1,2]</sup>. The Phasing Sensor is a Shack-Hartmann, with phasing sub-apertures positioned across the edge between adjacent segments. The initial procedure, called broadband phasing, consists of two tasks performed sequentially: the adjustment of the lateral position and rotation angle of the primary mirror image onto the lenslet array (registration) and the measurement of the surface discontinuity at the location of the phasing sub-apertures. This procedure has been tested at the GTC<sup>[3]</sup>. The tests demonstrated its capability to meet the E-ELT performance requirements. However, the procedure did not satisfy the operational requirements for its adaptation to the E-ELT context, where registration and phasing measurements need to be simultaneous and the overall procedure substantially faster (the standard procedure as implemented for the ESO experiment at the GTC takes about 1 hour for its final convergence phase). These specific E-ELT needs are justified in the next paragraph.

### 1.1 Registration requirements

According to models, which have been confirmed by on-sky tests, the tolerance for the registration error is of the order of 10mm, i.e. about 0.02% of the primary mirror diameter. With the E-ELT, thermo-mechanical deflections of the telescope structure prevent the system from maintaining passively this performance, even on a time scale of a few minutes. Simultaneous measurement of the registration while phasing is therefore required. An indirect method based on monitoring the photometry through sub-apertures across the edges of the primary mirror has been proposed<sup>[4]</sup>. The qualification “indirect” refers to the fact that the photometric signal is induced to the registration error but is not a direct measurement of the effect of the mis-registration on the response of a phasing sub-aperture. The bi-colour procedure described in the present paper performs a direct measurement of the registration parameters, while at the same time providing an update of the phasing solution.

In addition to thermo-mechanical deflections of the telescope structure, the deformations of the back structure holding the E-ELT primary mirror distort the segmentation pattern by up to  $\sim 5\text{mm}$ , a substantial fraction of the registration tolerance. This requires measuring not only the lateral pupil error but also its main deformation modes.

## 1.2 Timing requirements

The E-ELT requirement for a fast optical phasing procedure, capable of restoring the phasing solution in a few minutes was derived from two needs.

The on-sky phasing calibration of the Edge Sensors is a more demanding task at the E-ELT than on the existing 10m class segmented telescope. The differential in-plane motions of adjacent segments under gravity load reaches  $200\mu\text{m}$ . This couples to the Edge Sensors angular alignment errors ( $\delta\alpha$ ,  $\delta\beta$ ) with sensitivity  $\delta P = \delta G \delta\alpha + \delta S \delta\beta$ , where S and G are the displacements along the shear (parallel to inter-segment boundary) and gap (orthogonal to the inter-segment boundary) directions. S and G are measured by the Edge Sensors, but the coupling coefficients  $\delta\alpha$  and  $\delta\beta$  must be calibrated in-situ with an accuracy of  $\sim 0.1\text{mrad}$ . This implies a calibration effort consisting in repeating the optical phasing in various conditions to obtain the sensitivity coefficients. Moreover, the daily exchange of 1-2 segments needed to complete the primary mirror re-coating cycle within a duration of 18 months also implies a night to night update of the coupling coefficients.

The long-term stability of the Edge Sensors as specified for E-ELT, their sensitivity to temperature and humidity call for frequent update of the optical phasing during science operations.

In order to face the demanding registration and timing requirements at E-ELT, we developed and demonstrated at the GTC a fast optical phasing procedure meeting these requirements. This paper describes the procedure and reports on results obtained at the GTC.

## 2. PHASING SENSOR

### 2.1 Hardware Description

The baseline design of the Shack Hartmann lenslet array for E-ELT is an expansion of the GTC Segment Figure Sensor (SFS-2) probe to the E-ELT 798 segments configuration. It matches the segmentation of the primary mirror, with 19 inner sub-apertures per segment and 2 phasing sub-apertures across the edges between adjacent segments (figure 1). The phasing sub-apertures are composed of two parallel slits of width 45mm and length 120mm, separated by a 30mm wide mask. They provide diffraction-limited images up to a seeing of approximately 1 arc second. The focal plane sampling is 0.2 arc seconds per pixel and the field of view 4 arc seconds. The diffraction of the pupil image by the field stop results in a pupil resolution at the lenslet array comparable to the size of the sub-aperture. This reduces substantially the efficiency of the 30mm gap between the two slits, initially thought to mask the gap between the segments and the misfigure at the segment edges.

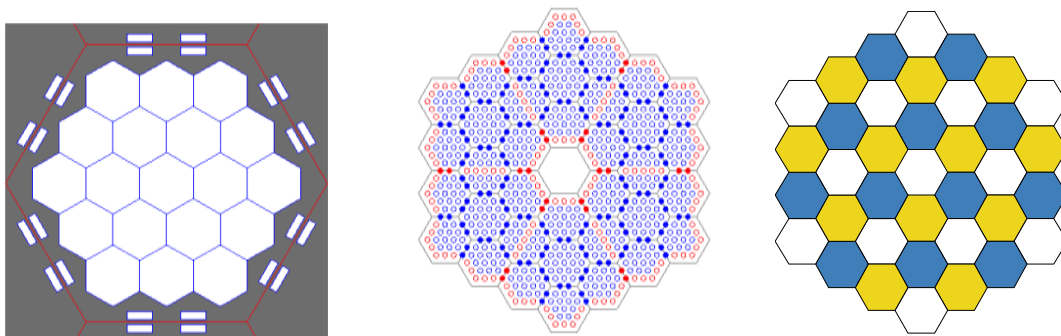


Figure 1: Geometry of the GTC Shack Hartman lenslet array. Left: the inner and phasing sub-apertures in one segment. Center: the pattern of inner (open circles) and phasing (filled circles) sub-apertures in the GTC phasing sensor SFS-2. The red circles indicate sub-apertures rejected from measurement for the data analyses (edge sub-apertures due to the M2 edge figuring errors on the outer edge and sub-apertures shadowed by the M2 spider arms). Right: the 3 segments families, defined such that any segment of one family is adjacent to segments from the 2 other families.

The sensor accommodates filters with different wavelengths and coherence lengths. The discontinuity at the segment edges, created by segment misfigure and/or phasing errors, induce a modulation of the PSF profiles, with an amplitude which depends both on the coherence (the ratio of the Optical Path Difference, or OPD, to the filter's coherence length) and on the registration error. The profile of the incoherent PSF depends also on the registration error (Figure 2).

Frames are integrated over 10 to 20 seconds in order to average the free atmosphere seeing. The phasing sub-apertures have a collective area about 6 times smaller than the inner sub-apertures. In addition, under sub-arcsec seeing, the phasing sub-apertures operate in diffraction limited conditions while the inner sub-apertures are seeing limited. This creates contrasts larger than 10 between the peak intensities of the 2 types of apertures. As the dynamic of the detector at GTC is limited to 14 bits, the integration time must be adapted to the star magnitude in order to avoid saturating in the inner sub-aperture, while reaching a decent SNR in the phasing sub-apertures.

## 2.2 Low level data reduction / sensor characterization

The spot centroids errors in the inner sub-apertures are measured with standard algorithms. For the phasing sub-apertures, the 1-dimensional PSF profiles are extracted by collapsing the 2-D image along the local edge direction with a Gaussian weighting function. The profiles are computed with the same sampling as the original image (0.2 arcsec / pixel) across a field of view of 6 arcsec (31 pixels).

An elementary set of measurements consists of 3 Shack Hartmann frames with  $\lambda/3$  piston steps (OPD) applied to each of the three segment families (Figure 1), using the position actuators of the segments. The three frames obtained with one filter are projected on the basis  $[1, \cos\varphi, \sin\varphi]$ , where  $\varphi$  is the phase applied at each step. The projection on the first component is the measured incoherent profile. The other two components form the phase modulation basis. The fringe contrast is defined as the ratio of the norm of the modulation basis to the norm of the incoherent profile.

The cosine and sine profiles are derived by determining the rotation angle  $\varphi_0$ , which maximizes the symmetry of the first component and the anti-symmetry of the second component relative to the central pixel of the profile. The extracted Incoherent, Cosine and Sine profiles are called the ICS profiles.

For the bi-colour phasing procedure, the narrow band filters for which the coherence is long (e.g.  $40\mu\text{m}$  for the  $650\pm 5\text{nm}$  filter) must be characterized by extracting the ICS profiles from elementary measurements taken at a series of registration positions (Figure 2). An analytical fit of the results provides for this filter and for each sub-aperture a model of its response to OPD and registration errors. The prerequisite for this calibration is that that phasing errors in the mirror are less than  $\sim 1\mu\text{m}$  (amplitude of the wavefront discontinuity, so that the fringe contrast depends only on the registration state. This prerequisite is achieved with the broadband phasing procedure.

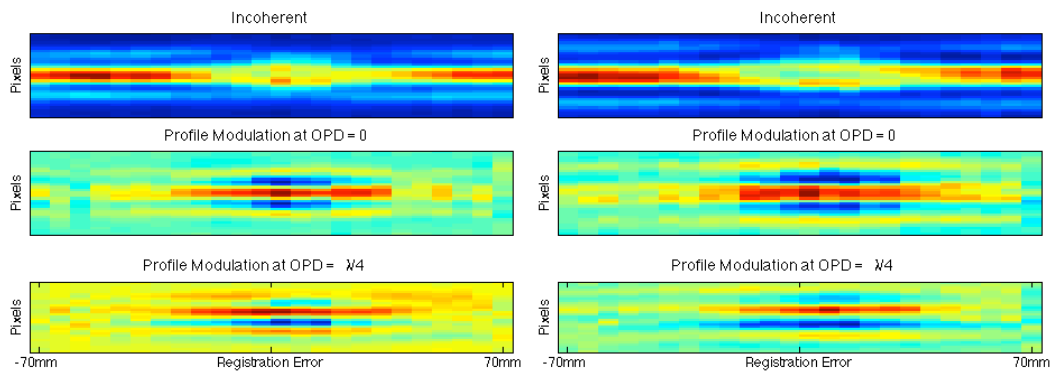


Figure 2: response of two filters to OPD and registration errors. The central wavelengths are 650nm (left) and 890nm (right). Both filters have a narrow optical bandwidth of 10nm, providing a large coherence length (respectively 40 and  $80\mu\text{m}$ ). For each filter, the top plot shows a waterfall display of the incoherent profiles for registration errors varying left to right from -70 to +70mm. The middle and bottom plots show the two modulation modes of the incoherent profiles induced by OPD between the 2 segments.

### 3. BROADBAND PHASING PROCEDURE

The broadband procedure consists of two steps, which are carried out sequentially: the registration between the sensor and the primary mirror and the phasing sequence.

#### 3.1 Incoherent registration

The sensor-to-primary mirror registration is an important prerequisite to the optical phasing, because alignment errors of the phasing sensor sub-apertures with respect to the mirror segments not only reduce the contrast of the fringes but also distorts the incoherent profiles, sometimes asymmetrically (Figure 2). This distortion is thought to be caused by imperfections in the Shack-Hartmann manufacturing, although this point has not been fully clarified.

The aim of the registration technique is to align the Shack-Hartmann lenslet array in translation and rotation to the image of the segmented primary. The incoherent registration procedure is performed with a broadband filter (e.g. 200nm bandwidth, centered at 700nm). The procedure starts by applying large piston steps to the segments, with amplitude larger than the coherence length of the filter, in order to guarantee that all phasing sub-aperture are operated in incoherent mode. Lateral offsets are sequentially applied to the image of the primary mirror in the three directions perpendicular to the segment edges. Along the scan, the footprint of one sub-aperture on the primary mirror transits from one segment to the other. As long as the twin footprints of a pair of subapertures cover a single segment, the PSF is the diffraction pattern of the pair of sub-apertures. During the transition, the PSF is the incoherent superposition of the diffraction patterns of each subaperture. This results in a sequence of profiles as in the top panel of Figure 2.

The data analysis consists in detecting for each sub-aperture the center of the transition along the scan. The vector of positions of the centers relative to the current pupil reference is fitted with a 4 parameters model (X and Y translation, rotation and scale).

The accuracy and duration of this procedure depend on the number of scan increments, the star brightness, and operational constraints. At GTC a typical standard registration template is executed within 40 minutes (mag 7, 51 steps, plus additional overheads to set large piston reference).

Since the procedure severely perturbs both the phasing and the registration, it cannot be concurrent with science observations.

#### 3.2 Broadband phasing

The broadband phasing procedure is carried out subsequently assuming that the pupil registration is not perturbed considerably. The procedure consists in applying piston steps between adjacent segments. At each position, an elementary set of measurements (3 frames with  $\lambda/3$  OPD offsets) is acquired. The resolution of the scan must sample the coherence length of the colour filter (9 points per coherence length was found experimentally to be satisfactory), and the total amplitude must be larger than the estimated phasing error.

The incoherent profiles and the phase modulation basis are then reduced to two numbers: the fringe contrast and the phase (obtained by projecting the modulation basis on a synthetic model). The evaluation of the OPD at the phasing sub-apertures combines two informations: the position of maximum fringe contrast indicates the position of the white fringe (stationary phase across the filter optical bandwidth). A standard atmospheric model computes the offsets between the white fringe and the 0 OPD, induced by the longitudinal chromatic dispersion in the direction of the guide star. At the GTC site altitude (2300m), when observing near the pole, the wrong fringe can be selected if this effect is not corrected. The phase of the profile modulation is used to determine the OPD with sub-wavelength accuracy.

In degraded conditions, e.g. after the installation of the segments in the mirror (accuracy  $\sim 200\mu\text{m}$ ), the procedure is performed with a narrow band filter (40 or  $80\mu\text{m}$  coherence length) with coarse resolution and over an amplitude of  $\pm 200\mu\text{m}$ . The procedure is then repeated with shorter coherence length and higher resolution. The last iteration uses the 700nm colour filter with 200nm bandwidth, whose coherence length is 2.4  $\mu\text{m}$ . Typical standard phasing templates are executed in 20 minutes (mag 7, 9 positions with 3 steps at each position).

The major shortcomings of the broadband phasing approach are its time overheads and the fact that it does not simultaneously evaluate the registration state. The long duration prevents this technique to be applied more frequently than about every two weeks. Due to the segment piston scan it cannot be applied in parallel to scientific observation. With the implementation of a bi-colour phasing approach described in the next section, the optical phasing can be done within a few minutes including registration control.

## 4. BI-COLOUR PHASING

Two innovations were brought to the standard procedure to allow a faster execution and evaluate simultaneously the registration parameters.

### 4.1 Use of long coherence filters

With an optical bandwidth of 10nm, the coherence length of the filter ranges from 40 to 80  $\mu\text{m}$  OPD for wavelengths of 650 and 890 nm, respectively. The fringe contrast in the phasing sub-apertures does not depend on the amplitude of the phasing error, provided that the amplitude of the wavefront discontinuities is within a few micrometres. The loss of contrast is therefore the signature of a local registration error. The contrast is measured twice with a controlled lateral shift of the pupil image between the two measurements. This breaks the symmetry of the response and allows determining the signed registration error by matching the measured ICS profiles to the calibrated sub-aperture model. For one sub-aperture, the accuracy of the measurement is poor, but combining together the measurements across the entire mirror allows determining the low order registration parameters (translation, scale, rotation).

### 4.2 Bi-colour measurements

With one filter, the phase is measured with  $2\pi$  ambiguity. Combining the measurements in two filters lifts this ambiguity. The dynamic range of the measurement is approximately the ratio of the product of the wavelengths to their difference. We opted for a  $4/3$  wavelength ratio, which provides a dynamic range equal to 3 waves of the redder filter, i.e.  $\sim 2.7 \mu\text{m}$ . This relatively large separation makes the fringe determination robust to phase measurement errors up to  $45^\circ$  in the bluer filter and  $60^\circ$  in the redder filter. It implies that the initial phasing error must remain within  $\pm 1.3 \mu\text{m}$  OPD, which translates in a capture range about 40 times the phasing performance requirement of the E-ELT, and therefore suitable to restore the phasing before the solution diverged from the specification by a large factor.

### 4.3 Bi-colour phasing procedure

2 pupil positions are used with offsets of -10 and +10mm relative to the reference, each with a different colour filter (650 and 890nm, both with a 10nm bandwidth). At each position, an elementary set of measurements is acquired (3 frames with  $\lambda/3$  piston steps between adjacent segments). All together, 6 frames are acquired. In the GTC implementation, the total duration of the procedure is about 5 minutes.

## 5. ELEMENTS OF THE DATA REDUCTION ALGORITHMS

This section describes the main steps of the data reduction procedures and algorithms (Figure 3). For clarity and concision, the evaluation of the measurement noise is not described. The measurement noise is used in the reconstruction of the mirror state so as to minimize its propagation.

### 5.1 Correction of reference pixels

For each frame the vector of centroid errors is projected onto a low order basis ( $\sim 100$  modes). The time series of modal coefficients are then used to estimate the static low orders, while the time variations are interpreted as a measurement of the dynamic wavefront errors during the acquisitions (slow components of free atmospheric seeing and dome/mirror seeing). The static part is kept for the evaluation of the segment stacking and shape errors and the dynamic part is used to compute for each frame the shift of the centroids induced by atmospheric turbulence at the locations of the phasing sub-apertures. The reference pixels in the phasing sub-apertures are offset accordingly.

### 5.2 Extraction of Profiles

A first evaluation of the segment stacking and shape errors is derived from the static centroid errors. This is used to compute the surface slopes at the positions of the phasing sub-apertures. There are two slope components ( $S_1$  and  $S_2$ ) per sub-aperture (one for each segment). They are combined as follows:

- the mean slope  $S_0 = (S_1 + S_2)/2$  is an additional offset to the sub-aperture reference pixel.
- the difference  $\delta S = (S_1 - S_2)/2$  will be used later when the registration parameters are determined.

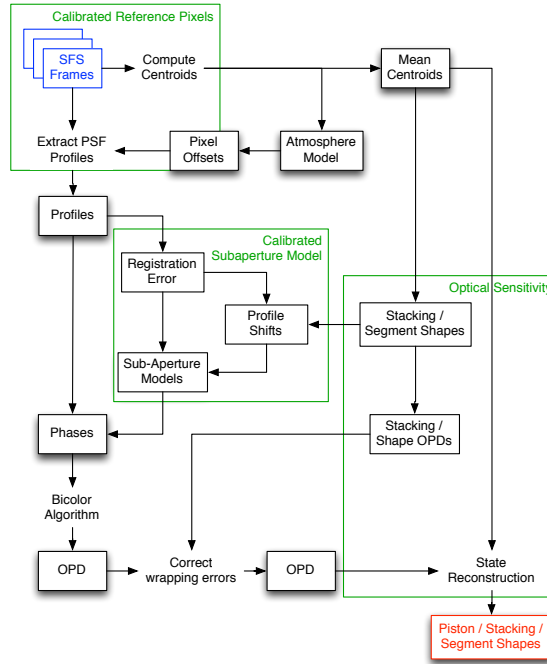


Figure 3: block diagram description of the bi-colour phasing data analysis procedures.

### 5.3 Evaluation of the registration error

Four registration parameters are estimated: the lateral error ( $\delta X$ ,  $\delta Y$ ), the rotation error ( $\delta\theta$ ), the scale error ( $\delta S$ ). They are determined by minimizing the fitting error of the measured ICS profiles on the calibrated sub-aperture models at the estimated registration state. The iterative method consists in following the gradient of the fitting error until a minimum is reached.

### 5.4 Phase measurements.

For each sub-aperture the ICS model of the library is extracted at the estimated registration state. The differential slope between the two adjacent segments at the location of the sub-aperture is compensated by shifting the ICS model by the angle  $\delta S \delta R \cdot G / w$ , where  $\delta R$  is the registration error at the sub-aperture location,  $G$  is the local gap unit vector and  $w = 60\text{mm}$  is the half-width of the sub-aperture.

The measured profiles are then projected on the ICS model. The second and third components are the cosine and the sine of the phase. The phase is estimated in the interval  $[-\pi, \pi]$ .

### 5.5 OPD estimation

The nominal relation between phase and OPD and the phases is:  $2\pi \text{OPD} = \varphi_1 \lambda_1 = \varphi_2 \lambda_2$ . The line with equation  $L = \varphi_1 \lambda_1 = \varphi_2 \lambda_2$  truncated to the OPD range  $\pm \lambda_1 \lambda_2 / (\lambda_1 - \lambda_2)$  wraps into the square  $[-\pi, \pi]^2$  to form the branches shown in figure 4. This branches are the locus of exact phase pairs within the capture range of the filter. The pairs of measured phases are projected onto the nearest position in this L line to determine the OPD. The dispersion of the phase pairs around the L line is an evaluation of the phase measurement noise.

### 5.6 Global reconstruction

The observables used in the reconstruction of the mirror state are:  $2 \times 19$  centroid errors in the inner sub-apertures of each segment, 2 OPD estimation in the phasing sub-aperture across the edge of each pair of adjacent segments, i.e. a maximum of 44 independent observables per segment (less for segments at the edge of the primary mirror). The fitted parameters are: the segment piston, tip-tilt, focus, astigmatism, coma and trefoil errors, i.e. 10 parameters per segment. The fit is obtained with the pseudo inverse of the interaction matrix between the fitted parameters and the observable.

Simulations have been used to synthesize the interaction matrix. With a ratio of more than 4 observables for 1 fitted parameter, the problem is thus strongly over-constrained, which allows estimating a posteriori the measurement noise.

## 6. RESULTS

The bi-colour phasing procedure was tested during 2 technical runs at the GTC, in February and May 2014. It was found to perform optimally for sub-arcsec seeing and remain robust for seeing up to about 1.2 arc seconds. This limit is consistent with the characteristics of the subapertures.

### 6.1 Registration

The fast registration procedure converges even with a substantially degraded initial state (40mm as projected on the primary mirror). At E-ELT, this initial condition can be reached by photometric methods comparing the flux through sub-apertures positioned across the edge of the mirror at different azimuth positions. The repeatability of the measurement after convergence indicates an accuracy better than 5mm.

### 6.2 Phasing

The centroid noise is estimated from the frame-to-frame measurement variations after subtraction of the estimated residual atmospheric noise. Under sub-arcsec seeing condition, the noise level is 20 milli-arc seconds, i.e. 0.1 pixel, a standard performance. The OPD noise is estimated from the repeatability of the measurements (10 consecutive templates were executed at a constant elevation angle, under sub-arc second seeing condition). The standard deviation of the OPD measurements is 15nm.

The consistency of the phase measurements in the two filters is also an indicator of the phase measurement noise. An example obtained in sub-arcsec seeing condition is shown in Figure 4, where the quadratic mean of the distance of the pairs of phase measurement to their nominal locus is 12 deg, i.e. 20nm in the shorter filter. This number was brought down to 8 degrees with excellent seeing conditions (0.6 arcsec) during the May campaign.

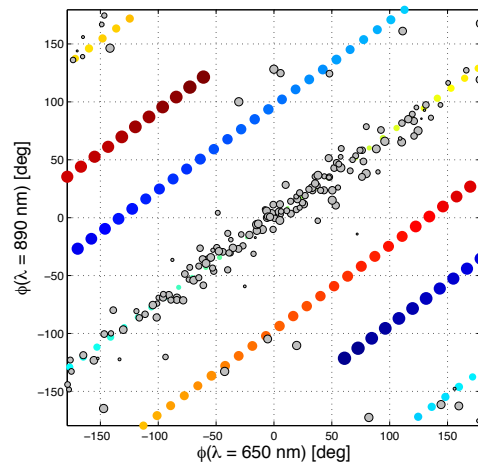


Figure 4: Bi-colour phase measurements: the aligned coloured spots form the wrapped branches of the line  $L$  defined by the equation  $\varphi_1 \lambda_1 = \varphi_2 \lambda_2$  where pairs of exact phase measurements would be found. The gray dots are the measurements obtained in the 168 sub-apertures of the GTC phasing sensor. The diameter of the spot indicate the weight with which they contribute to the reconstruction of the mirror state. The large dispersion of the data in the OPD direction is the signatures of the wavefront discontinuities created by the segment shape errors, which were not corrected in this experiment.

As the reconstruction problem is over constrained, the analysis of the consistency of the fitting error with the estimated noise level provides an estimation of the differential measurement biases. This was found to be 50nm in OPD space, but we cannot evaluate how this breaks down between OPD and centroid biases.

Another way of evaluating the noise propagation is to compare the solutions found in consecutive measurements taken in similar conditions (Figure 5). The amplitude of the differential measured surface errors is twice larger and projects on spatial orders lower than expected from the noise propagation analysis. This is interpreted as an indication that the

system reached the regime where the performance is limited by the residual dynamic error at the time scale of the measurements (residual atmospheric seeing, mirror seeing, mirror dynamic). This was confirmed in the May run, where lower residual (60 to 80nm) were found under excellent seeing conditions (0.6 arcsec).

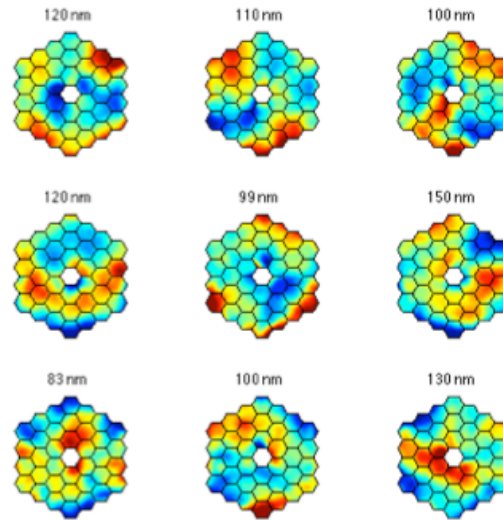


Figure 5: differential surface reconstruction in 9 consecutive phasing measurements. The mean reconstructed surface error has been subtracted from the maps.

## 7. CONCLUSION

The test campaigns at the GTC demonstrated that the bi-colour phasing procedure can be executed in 5 minutes and restore the phasing solution. As the 6 frames acquired in the procedure form a non redundant set of data for the simultaneous measurement of the registration and phasing errors, the worst seeing across the data set limits the accuracy. Measurements collected in different seeing conditions indicate that the procedure remains robust up to peak seeing values of 1.2 arc-second.

The procedure measures the registration error while acquiring the phasing data. The estimated registration error is incorporated in the fitting model used to measure the phase. This was found to increase the robustness to registration errors. The limiting factor to the registration performance is now the loss of fringe contrast. The procedure was found to be robust to registration errors of 40mm.

With the selected wavelengths, the capture range of the procedure is  $\pm 1.3\mu\text{m}$  wavefront discontinuities. The procedure is therefore valid to restore the phasing only if the initial state of the mirror is within this range. For more degraded condition, the standard broadband procedure remains the baseline. With the E-ELT, in-situ metrology is an option considered as part of the segment exchange process. This capture range directly feeds into the requirements of such metrology, whose concept still needs development and is not covered herein.

For E-ELT, the bi-colour phasing procedure provides an efficient method for the in situ characterization of the edge sensors for which a large number of optical phasing must be performed at various elevation angles. In addition, it opens the possibility to optimizing the phasing solution at the beginning of an observation particularly demanding in performance.

## ACKNOWLEDGMENT

The results reported in this paper were based on observations made with the Gran Telescopio Canarias (GTC), installed in the Spanish Observatorio del Roque de los Muchachos of the Instituto de Astrofísica de Canarias, in the island of La Palma. These observations were made under the scope of the Agreement for ESO Technical Access to GTC.

The authors wish to thank Javier Castro and the GTC operations team for their remarkable support.



## REFERENCES

- [1] Gary Chanan, Mitchell Troy, Frank Dekens, Scott Michaels, Jerry Nelson, Terry Mast, and David Kirkman, "Phasing the Mirror Segments of the Keck Telescopes: The Broadband Phasing Algorithm," *Appl. Opt.* 37, 140-155 (1998)
- [2] Gary Chanan, Catherine Ohara, and Mitchell Troy, "Phasing the Mirror Segments of the Keck Telescopes II: The Narrow-band Phasing Algorithm," *Appl. Opt.* 39, 4706-4714 (2000)
- [3] P. Álvarez ; J. Castro ; R. Rutten ; M. van der Hoeven ; C. Álvarez and A. M. Perez-García, "The GTC project: from commissioning to regular science operation. Current performance and first science results", *Proc. SPIE 7733, Ground-based and Airborne Telescopes III*, 773305 (July 28, 2010);
- [4] Piotr Piatrou and Gary Chanan, "Shack–Hartmann mask/pupil registration algorithm for wavefront sensing in segmented mirror telescopes," *Appl. Opt.* 52, 7778-7784 (2013)